

## The crystal structure of “Tetragonal Almandine-Pyrope Phase” (TAPP): A reexamination

LARRY W. FINGER\* AND PAMELA G. CONRAD†

Geophysical Laboratory and Center for High Pressure Research, 5251 Broad Branch Road N.W., Washington, D.C. 20015-1305, U.S.A.

### ABSTRACT

X-ray intensities for the “tetragonal almandine-pyrope phase” (TAPP),  $*(\text{FeMg})^{\text{VIII}}(\text{AlMgFe})_4[\text{IV}(\text{SiAl})\text{O}_4]_3$ , where \* refers to a capped tetrahedral site, reported by Harris et al. (1997) were recollected using the identical crystal, and the crystal structure was refined from these new data. The basic structure of the previous report is confirmed; however, some of the details regarding cation occupancies are revised. The chemical composition of this phase corresponds to a high-pressure origin; however, significant questions remain regarding the crystallization pressure of this phase.

### INTRODUCTION

Inclusions in diamonds have been used for many years to study the mineralogy and pressure-temperature conditions of the mantle (e.g., Futergendler 1969; Harris 1969, Meyer and Boyd 1972; Sobolev et al. 1974; Meyer and Tsai 1979; Harte et al. 1980; Hervig et al. 1980; Gurney 1986; Meyer 1987; Kesson and Fitzgerald 1992). The vast majority of inclusions contain phases that have been observed in natural rocks, or have been synthesized in phase-equilibria studies; however, a new phase was found in eight diamonds from São Luiz, Brazil (Harte and Harris 1994). This phase, which has a composition close to the pyrope-almandine join, was given the acronym TAPP, for tetragonal almandine-pyrope phase. This material was studied with X-ray diffraction by Harris et al. (1997) and with Mössbauer spectroscopy by McCammon et al. (1997).

Since publication of the original report on the crystal structure, the synthesis of an isostructural phase  $*(\text{Mg,Fe})_{0.85}^{\text{VIII}}(\text{Mg,Fe})_4[\text{IV}(\text{Fe,Ge})\text{O}_4]_3$  was reported (Lévy and Barbier 2000), where \* denotes the capped tetrahedral site. In addition, this structure is also found for  $*(\text{Na,Mg})^{\text{VIII}}\text{Mg}_4(\text{IVVO}_4)_3$  (Murashova et al. 1988),  $*\text{Mg}_{0.5}^{\text{VIII}}\text{Mg}_4(\text{IVAsO}_4)_3$  (Krishnachari and Calvo 1973),  $*\text{Co}_{0.5}^{\text{VIII}}\text{Co}_4(\text{IVAsO}_4)_3$  (Gopal et al. 1980), and  $*\text{Ni}_{0.5}^{\text{VIII}}\text{Ni}_4(\text{IVAsO}_4)_3$  (J. Barbier personal communication 1999). The present study was undertaken to confirm the crystallographic results of Harris et al. (1997) and to discuss the implications of the occurrence of TAPP, particularly in view of these isostructural materials.

### DATA COLLECTION

We mounted the pale green crystal studied by Harris et al. (1997) on a Bruker P4 four-circle diffractometer with a SMART 1000 CCD detector employing Mo  $K_\alpha$  radiation and the generator set at 50 kV, 40 ma. A hemisphere of data to 0.7 Å was collected with 0.3 degree frames. Counting time for each frame

was 60 sec. These data were corrected for geometrical distortion, dark current and flood-field deviations using the normal software. After indexing, integrated intensities were extracted using Bruker software. The resulting data were corrected for Lorentz and polarization effects. Merging of the data, both for redundant reflections and the symmetrical equivalents were completed with program XPREP from the Bruker SHELXTL package. No absorption correction was undertaken. Crystal structure refinement was completed with the RFINE90 suite of programs (Finger and Prince 1975).

The very high sensitivity of the CCD detector and the ability to sample background in all three directions in reciprocal space make this instrument very useful for the study of small and/or weakly diffracting crystals (Burns 1998). Although the size of the crystal is generally emphasized, a more important measure is the intrinsic scattering power of the crystal, which is defined as  $S = (F_{000}/V_U)^2 V_C \lambda^3$ , where  $F_{000}$  is the number of electrons in the unit cell,  $V_U$  is the volume of the unit cell,  $V_C$  is the volume of the crystal, and  $\lambda$  is the wavelength of the experiment. For a typical laboratory single-crystal diffractometer with a point detector,  $S \approx 10^{17}$ . In the present study, the size of the crystal (Table 1) yields  $S = 3.9 \times 10^{16}$ , thus the TAPP study was not particularly difficult for the CCD system. A total of 355 symmetry-independent intensities were measured. Of these, 326 had structure factors that were greater than twice the standard deviation, see Table 1.

### REFINEMENT RESULTS

Preliminary refinements of the crystal structure of TAPP indicated that the structure of Harris et al. (1997) is basically correct. The new crystallographic data are in Tables 1 and 2. The computer program SHELXS, which is part of the Bruker program package was used to solve the crystal structure. The topology is as reported by Harris et al. (1997), with five distinct cation positions. Two of these (T1, T2) are tetrahedrally coordinated by oxygen, two (M2, M3) are octahedrally coordinated, and the last (M1) is a site of  $\bar{4}$  symmetry, which generates a capped tetrahedron with four shorter and four longer bonds. The general formula for this structure could be written as  $\text{M}^*\text{M}_4(\text{TO}_4)_3$ , where M is an octahedral cation site, T is a

\* Current address: 1400 Colorado St., Boulder City NV 89005; E-mail: Larry.Finger@tcw.net

† Current Address: Jet Propulsion Laboratory, 4800 Oak Grove Drive, Pasadena CA 91009.

tetrahedral site, and M\* is the capped tetrahedral site. In  $^*\text{Mg}_{0.5}^{\text{VIII}}\text{Mg}_4(\text{IVAsO}_4)_3$  (Krishnachari and Calvo 1973),  $^*\text{Co}_{0.5}^{\text{VIII}}\text{Co}_4(\text{IVAsO}_4)_3$  (Gopal et al. 1980), and  $^*\text{Ni}_{0.5}^{\text{VIII}}\text{Ni}_4(\text{IVAsO}_4)_3$  (J. Barbier personal communication 1999), the M\* site is 50% occupied, and has 85% occupation in  $^*(\text{Mg,Fe})_{0.85}^{\text{VIII}}(\text{Mg,Fe})_i[\text{IV}(\text{Fe,Ge})\text{O}_4]_3$  (Lévy and Barbier 2000). Only in TAPP and  $^*\text{Na}^{\text{VIII}}\text{Mg}_4(\text{IVVO}_4)_3$  (Murashova et al. 1988) is there nearly complete occupancy of M\*. For the latter material, the two distances from M\* to O are 2.36 and 2.68 Å; therefore, the site becomes more nearly cubic coordinated, as might be expected for Na. Note that there is a difference in the atom naming conventions and the choice of origin between TAPP and the isostructural compounds of Krishnachari and Calvo (1973), and Gopal et al. (1980). The origin is shifted by (0,0,1/2), with the following transformation in site names from TAPP to the other structures: T1 → T2, T2 → T1, M1 → M3, M2 → M1, M3 → M2, O1 → O2, O2 → O3, and O3 → O1. For easy comparison of our results with those of Harris et al. (1997), their conventions are used here. Note that Murashova et al. (1988) use the shifted origin relative to TAPP, but have a third, distinct atom naming convention.

For purposes of refinement, the composition could be simplified to  $\text{Fe}'_{1.96}\text{Mg}'_{10.60}\text{Al}_{7.76}\text{Si}_{11.64}\text{O}_{48}$ , where Fe' is  $\text{Fe}^{2+} + \text{Fe}^{3+} + \text{Mn} + \text{Cr} + \text{Ca}$ , and Mg' is  $\text{Mg} + \text{Na}$ . Note that this formula deviates by only 0.04 from the fully occupied ratio of 32 cations to 48 anions, thus the M1 site is fully occupied. In this refinement, this deficiency was assumed to occur in the Mg or Na. Cation assignments were made as follows: (1) Based on mean T-O distances, T1 is fully occupied by Si. (2) T2 contains the remaining Si with Al added to reach 100% occupancy. (3) The remaining Al is placed in M2 based on average M-O dis-

tances. (4) Mg' and Na are distributed over M1 and M3, and (5) the remaining cations are found on all three M sites. The occupancy of Fe' on these sites, which is the only variable allowed under these assumptions, was refined subject to a bulk composition constraint. Statistics for the resulting refinement are shown in Table 1, with the structural parameters displayed in Table 2. The temperature factors for this model were more realistic than for the model proposed by Harris et al. (1997), even though the occupancies are nearly identical.

The current experiment is only sensitive to the total number of electrons in each site, which has no unique solution for the complicated chemistry. We can, however, make several conclusions based on these results. The first is that there is no evidence for vacancies in any of the cation sites, a result that differs from that reported by Harris et al. (1997). A second result is that very little, if any, Fe occurs in T1 or T2 as argued by Harris et al. (1997). McCammon et al. (1997) found that  $\text{Fe}^{3+}$  had hyperfine parameters that were consistent with "either a tetrahedral site, or a distorted octahedral site." They concluded, based on stoichiometry and in agreement with the present results, that the latter possibility seems more likely. The scattering power of the T sites does not rule out the possibility of octahedrally coordinated Si with additional  $\text{IVAl}$ . Such an amount must be minor, as the mean T1-O distance is very near to the value expected for pure Si in isolated tetrahedra. In the ordered, isostructural phases  $^*\text{Mg}_{0.5}^{\text{VIII}}\text{Mg}_4(\text{AsO}_4)_3$  (Krishnachari and Calvo 1973) and  $^*\text{Co}_{0.5}^{\text{VIII}}\text{Co}_4(\text{AsO}_4)_3$  (Gopal et al. 1980), the  $\langle \text{T2-O} \rangle / \langle \text{T1-O} \rangle$  are 1.008 and 1.004, respectively. In the present study, this ratio is 1.006; therefore, there is no indication that T2 contains any more Al than the 4.5% required by stoichiometry. In addition, the mean-square amplitudes of vibration of the T atoms in the direction of the coordinating O atoms, as compared with the amplitudes of the oxygen vibration in the direction of the T ions, do not show any major effects of positional disorder due to substitution of Al for Si (Downs et al. 1990).

Note that the amount of Fe' in M1 (0.21) is nearly identical to the amount of  $\text{Fe}^{3+}$  (0.19) in the chemical analysis, which correlates with the Mössbauer results of McCammon et al. (1997), whose hyperfine parameters could be appropriate for this capped tetrahedron. From these results, it is likely that  $\text{Fe}^{3+}$  occurs in M1, and that  $\text{Fe}^{2+} + \text{Mn} + \text{Cr} + \text{Ca}$  is split between M2 and M3. McCammon et al. (1997) suggested that M2 was too small to satisfy the hyperfine parameters; therefore, Cr may be concentrated in M2. Furthermore, if  $\text{Fe}^{2+}$  were in both M2 and M3, charge transfer effects would make the color of the crystals much darker than is observed.

Although Harris et al. (1997) describe this tetragonal al-

TABLE 1. Crystal data and results of refinement for TAPP

Crystal size	$0.06 \times 0.04 \times 0.04 \text{ mm}^3$
Space group	$I\bar{4}2d$
Unit-cell dimensions at 26 °C	
a (Å)	6.5269(4)
c (Å)	18.1835(14)
V (Å <sup>3</sup> )	774.6(2)
X-ray density, g/cm <sup>3</sup>	3.581
Linear absorption coefficient, cm <sup>-1</sup>	18.72
MoK $\alpha$ radiation, wavelength (Å)	0.7107
Minimum d (Å) collected	0.7
Number reflections collected	7201
Number unique reflections	355
$R = \Sigma  F_o - F_c  / \Sigma  F_o $	0.024
$WR = \Sigma w(F_o - F_c)^2 / \Sigma (w F_o^2)$	0.016
Number with $F > 2 \sigma_F$	326
R	0.019
WR	0.016

TABLE 2. Atomic positions and thermal factors\* for TAPP

Atom	Site	Occupancy	x	y	z	$B_{\text{eq}}$ (Å <sup>2</sup> )	$B_{11}$	$B_{22}$	$B_{33}$	$B_{12}$	$B_{13}$	$B_{23}$
T1	4b	Si	1/2	1/2	0	0.41(2)	0.37(3)	= $B_{11}$	0.49(4)	0	0	0
T2	8d	0.955 Si + 0.045 Al	-0.1499(1)	1/4	1/8	0.44(1)	0.50(3)	0.42(3)	0.41(3)	0	0	0
M1	4a	0.210(7) Fe' + 0.790(7) Mg'	0	0	0	0.79(3)	0.70(4)	= $B_{11}$	0.96(6)	0	0	0
M2	8d	0.074(3) Fe' + 0.926(3) Al	0.2599(1)	1/4	1/8	0.51(2)	0.59(3)	0.52(3)	0.42(4)	0	0	0
M3	8c	0.066(5) Fe' + 0.934(5) Mg'	0	1/2	-0.02296(6)	0.55(3)	0.59(4)	0.51(4)	0.56(4)	0.04(3)	0	0
O1	16e	O	0.0187(3)	0.2809(3)	0.0576(1)	0.59(3)	0.47(6)	0.66(7)	0.63(6)	-0.11(6)	0.14(5)	0.14(5)
O2	16e	O	-0.2614(3)	0.0372(2)	0.1013(1)	0.73(3)	0.85(6)	0.57(6)	0.76(6)	-0.07(5)	-0.05(5)	-0.05(5)
O3	16e	O	0.4368(3)	0.2961(2)	0.0468(1)	0.65(3)	0.83(6)	0.48(7)	0.65(7)	-0.00(5)	0.05(5)	0.05(5)

\* All atoms refined with anisotropic thermal parameters of the form:  $T = \exp\{-\Sigma \Sigma h_i h_j B_{ij} a_i^* a_j^* / 4\}$ , where  $a_i^*$  is a reciprocal axis length and  $h_i$  is a Miller index.

mandine-pyropite phase in terms of its relationship to garnet based on stoichiometry, there is little relationship between this structure and that of a garnet. In garnet, the structure can be described as a framework of corner-linked tetrahedra and octahedra (Hazen et al. 1996) with a large, dodecahedral site. The structure of TAPP has edges shared between T2 and M2, and M1 and M2. Figure 1a shows details of the shared edges, and Fig. 1b shows the complete structure for TAPP. Selected bond distances and angles are shown in Table 3. The effects on the coordination polyhedra due to the edge sharing between T2 and M2 are most clearly noted in the angular variance (Robinson et al. 1971) for T2. On the other hand, M2 is very nearly a regular octahedron.

### DISCUSSION

The basic details of the crystal structure for TAPP presented by Harris et al. (1997) are confirmed; however, some of the details of cation occupancy have been clarified. In particular, we find no evidence for vacancies on any of the cation sites, nor for  $\text{Fe}^{3+}$  replacing Si or Al in tetrahedral coordination. We also find one of the tetrahedral sites to be completely occupied by Si, with approximately 5% of Al substituting into the other T site. There is no evidence for Si in octahedral coordination. The distorted M1 site, which is a capped tetrahedron, contains the  $\text{Fe}^{3+}$ , whereas  $\text{Fe}^{2+}$  is concentrated in M3. The M2 site is occupied by Al and Cr.

As noted by Harris et al. (1997), TAPP represents a chemical composition consistent with lower mantle pressure-temperature-path. The question as to whether this phase crystallized at high pressure remains. To be sure, it was found inside a diamond, which would seem to imply a high-pressure origin. However, is an edge shared between a tetrahedron and an octahedron likely to be stable to very high pressure? In the isostructural arsenates and vanadate, the ratio of the size of the octahedron to that of the tetrahedron for those polyhedra involved in the shared edge ranges between 1.225 and 1.235. For Mg-rich olivine (Brown 1980), a phase that contains edges shared between tetrahedra and octahedra and is stable to modest pressure, the equivalent parameter has a value of about 1.3. In TAPP, this value is only 1.17. The compressibility ratio between octahedron and tetrahedron is greater than unity; therefore, high pressure would tend to reduce this number. Does this low value in TAPP result from a high-pressure origin, or is it a simple con-

sequence of M2 occupancy by Al and Cr? Elasticity data could potentially resolve this.

If TAPP is a high-pressure phase, why do we not find some of the silicon in octahedral coordination? Of course, this finding is model dependent; however, the evidence is very strong. A counter argument is that germanate phases crystallized at room pressure can be isostructural with silicates stable at much higher pressure. Therefore, the phase of Lévy and Barbier (1998) may indicate a stability for TAPP at pressures greater than ambient.

One additional question to be addressed is why TAPP only occurs in diamonds from Brazil. Is it possible that the  $P$ - $T$  path of the emplacement of these diamonds differs from other cratons, and that the presence of TAPP reflects this history? In the laboratory, essentially all experiments are quenched by reducing temperature, then reducing the pressure. However, for diamonds, pressure-temperature paths may be complex. As a result, solid-state reactions could occur during the ascent of the diamond to the surface. A paragenesis of this type for TAPP would explain why it has not been synthesized in the laboratory.

After consideration of these factors, we suggest, but cannot prove, that TAPP crystallized during the ascent of the host diamond, rather than having a high-pressure origin. Clearly, additional phase equilibrium studies in the system  $\text{SiO}_2\text{-Al}_2\text{O}_3\text{-MgO}$ , possibly with  $\text{Fe}_2\text{O}_3$ , must be pursued to determine the stability of this phase. To aid the identification, Table 4 shows calculated  $d$  spacings and powder-pattern intensities calculated from the refined structure.

TABLE 3. Selected bond distances for TAPP

Bond	Distance (Å)	Bond	Distance (Å)
T1 - O3 (4×)	1.633(2)	M2 - O1 (2×)	2.005(2)
T1 - Quad. El.	1.0093	M2 - O2 (2×)	1.923(1)
T1 - Ang. Var.	34.85	M2 - O3 (2×)	1.857(2)
		Mean M2 - O	1.928
T2 - O1 (2×)	1.659(2)	M2 - Quad. El.	1.0107
T2 - O2 (2×)	1.626(2)	M2 - Ang. Var.	33.96
Mean T2 - O	1.642		
T2 - Quad. El.	1.0282	M3 - O1 (2×)	2.051(2)
T2 - Ang. Var.	116.7	M3 - O2 (2×)	2.125(2)
		M3 - O3 (2×)	2.023(2)
M1 - O1 (4×)	2.115(2)	Mean M3 - O	2.066
M1 - O2 (4×)	2.523(2)	M3 - Quad. El.	1.0214
Average of 8	2.319	M3 - Ang. Var.	70.60

Notes: Quadratic elongation and angular variance are defined by Robinson et al. (1971).

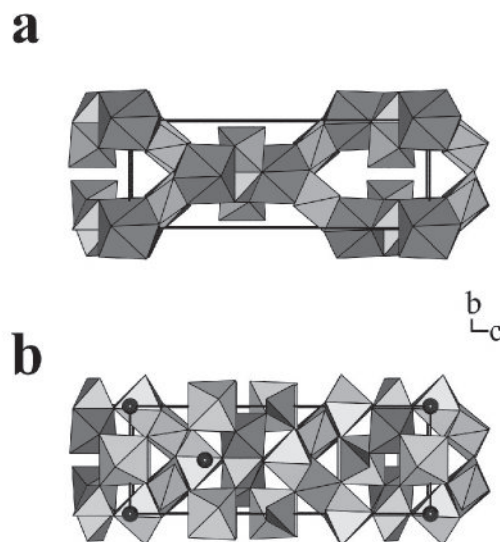


FIGURE 1. Views of the crystal structure of TAPP. (a) The edges shared among the T2 tetrahedron, the M2 octahedron, and the M1 polyhedron, and (b) the complete structure. In this view, the M1 cation is represented by the large spheres, M2 and M3 are the darker and lighter octahedra, respectively, and T1 and T2 are the darker and lighter tetrahedra, respectively.

TABLE 4. Calculated *d* values and intensities for TAPP

<i>h</i>	<i>k</i>	<i>l</i>	<i>d</i> , Å	Int	<i>h</i>	<i>k</i>	<i>l</i>	<i>d</i> , Å	Int
1	0	1	6.1423	2	2	1	11	1.4383	3
0	0	4	4.5455	3	4	0	6	1.4365	1
1	1	2	4.1148	3	4	2	4	1.3894	12
1	0	5	3.1765	12	2	0	12	1.3742	7
2	0	2	3.0712	4	3	3	6	1.3716	5
2	1	1	2.8816	16	1	0	13	1.3676	3
2	0	4	2.6507	100	3	1	10	1.3642	2
2	1	3	2.6295	12	3	2	9	1.3481	1
1	1	6	2.5330	3	4	0	8	1.3254	3
2	2	0	2.3073	1	3	0	11	1.3161	1
2	1	5	2.2761	5	4	2	6	1.3148	4
2	0	6	2.2205	19	5	1	0	1.2799	3
3	1	0	2.0637	2	5	0	3	1.2760	1
2	2	4	2.0574	3	4	3	3	1.2760	1
3	0	3	2.0474	1	2	2	12	1.2665	2
3	1	2	2.0125	4	1	1	14	1.2502	1
2	1	7	1.9403	5	4	1	9	1.2459	1
1	0	9	1.9299	3	5	1	4	1.2320	1
3	1	4	1.8791	1	5	0	5	1.2285	3
3	0	5	1.8668	1	4	0	10	1.2143	1
2	0	8	1.8650	1	5	2	1	1.2092	1
3	2	1	1.8011	4	2	0	14	1.2067	1
3	2	3	1.7343	1	5	2	3	1.1883	1
3	1	6	1.7057	7	5	1	6	1.1790	1
1	1	10	1.6916	1	4	4	0	1.1536	1
2	1	9	1.6611	3	5	2	5	1.1497	1
4	0	0	1.6315	18	4	1	11	1.1432	1
3	2	5	1.6204	14	2	1	15	1.1194	1
2	2	8	1.6192	12	5	3	0	1.1192	1
1	0	11	1.6023	4	4	4	4	1.1182	1
3	1	8	1.5278	1	5	1	8	1.1152	1
3	3	2	1.5166	4	5	3	2	1.1108	1
0	0	12	1.5152	1	4	0	12	1.1102	1
3	2	7	1.4850	7	3	2	13	1.1067	1
3	0	9	1.4803	3	3	1	14	1.0992	1
4	2	0	1.4593	3	5	2	7	1.0982	1
4	1	5	1.4513	2	4	3	9	1.0963	1
4	2	2	1.4408	1	5	0	9	1.0963	1

## ACKNOWLEDGMENTS

This study was supported by NSF grants EAR9218845 and EAR9805282, and by the Carnegie Institution of Washington. The CCD diffractometer was purchased with NSF grant EAR9725354, with matching funds from the W. M. Keck Foundation. Constructive reviews by R.M. Hazen and C.T. Prewitt contributed a great deal to the final manuscript.

## REFERENCES CITED

- Brown, G.E. Jr. (1980) Olivines and silicate spinels. *Reviews in Mineralogy*, 5, 275–381. Mineralogical Society of America, Washington, D.C.
- Burns, P.C. (1998) CCD area detectors of X-rays applied to the analysis of mineral structures. *The Canadian Mineralogist*, 36, 847–853.
- Downs, R.T., G.V. Gibbs, and M.B. Boisen, Jr. (1990) A study of the mean-square displacement amplitudes of Si, Al, and O atoms in framework structures: Evidence for rigid bonds, order, twinning, and stacking faults. *American Mineralogist*, 75, 1253–1267.
- Finger, L.W. and E. Prince (1975) A system of Fortran IV computer programs for crystal structure computations. National Bureau of Standards (U.S.) Technical Note 854, 133 p.
- Futergendler, S.I. (1969) X-ray investigation of a natural diamond with garnet inclusions in the form of a crystallized silicate melt. *Soviet Physics Crystallography* 14, 248–251.
- Gopal, R., Rutherford, J.S., and Robertson, B.E. (1980) Closest Packing in Dense Oxides: The Structure of a Polymorph of Co<sub>3</sub>(AsO<sub>4</sub>)<sub>2</sub>. *Journal of Solid State Chemistry*, 32, 29–40.
- Gurney, J.J. (1986) Their Mantle/Crust Setting, Diamonds, and Diamond Exploration. In J. Ross, Ed., *Kimberlites and Related Rocks*, vol. 2, p. 935–965.
- Harris, J. (1969) Syngenetic mineral inclusions in diamond as identified by X-ray analysis. *Journal of Gemology*, 11, 256–262.
- Harris, J., Hutchison, M.T., Hursthouse, M., Light, M., and Harte, B. (1997) A new tetragonal silicate mineral occurring as inclusions in lower-mantle diamonds. *Nature*, 387, 486–488.
- Harte, B., Gurney, J.J., and Harris, J.W. (1980) The formation of peridotitic suite inclusions in diamonds. *Contributions to Mineralogy and Petrology*, 72, 181–190.
- Harte, B. and Harris, J.W. (1994) Lower mantle mineral associations preserved in diamonds (abstract). *Mineralogical Magazine*, 58A, 384–385.
- Hazen, R.M., Downs, R.T., and Finger, L.W. (1996) High-pressure framework silicates. *Science*, 272, 1769–1771.
- Hervig, R.L., Smith, J.V., Steele, I.M., Gurney, J.J., Meyer, H.O.A., and Harris, J.W. (1980) Diamonds; minor elements in silicate inclusions; pressure-temperature implications. *Journal of Geophysical Research*, B, 85, 6919–6929.
- Kesson, S.E. and Fitzgerald, J.D. (1992) Partitioning of MgO, FeO, NiO, MnO and Cr<sub>2</sub>O<sub>3</sub> between magnesian silicate perovskite and magnesiowuestite; implications for the origin of inclusions in diamond and the composition of the lower mantle. *Earth and Planetary Science Letters*, 111, 229–240.
- Krishnamachari, N. and Calvo, C. (1973) Magnesium arsenate, Mg<sub>3</sub>As<sub>2</sub>O<sub>8</sub>. *Acta Crystallographica*, B29, 2611–2613.
- Lévy, D. and Barbier, J. (2000) <sup>viii</sup>(Mg,Fe)<sub>0.85</sub><sup>vi</sup>(Mg,Fe)<sub>1</sub><sup>iv</sup>(Fe,Ge)<sub>3</sub>O<sub>12</sub>: A new tetragonal phase and its comparison with garnet. *American Mineralogist*, 85, 1053–1060.
- McCammon, C.A., Hutchinson, M., and Harris, J. (1997) Ferric iron content of mineral inclusions in diamonds from Sao Luiz; a view into the lower mantle. *Science*, 278, 434–436.
- Meyer, H.O.A. (1987) In P.H. Nixon, Ed., *Mantle Xenoliths*, p. 501–552. Wiley, Chichester, U.K.
- Meyer, H.O.A. and Boyd, F.R. (1972) Composition and origin of crystalline inclusions in natural diamonds. *Geochimica et Cosmochimica Acta*, 36, 1255–1273.
- Meyer, H.O.A. and Tsai, H.M. (1979) Inclusions in diamond and the mineral chemistry of the upper mantle. *Physics and Chemistry of the Earth*, 11, 631–644.
- Murashova, E.V., Velikodnyi, Y.A. and Trunov, V.K. (1988) Crystal structure of NaMg<sub>4</sub>(VO<sub>4</sub>)<sub>3</sub>. *Zhurnal Strukturnoi Khimii*, 29, 182–184.
- Robinson, K., Gibbs, G.V. and Ribbe, P.H. (1971) Quadratic elongation: a quantitative measure of distortion in coordination polyhedra. *Science*, 172, 567–570.
- Sobolev, V.S., Sobolev, N.V., and Lavrent yev Yu, G. (1974) Inclusions in diamond from diamondiferous eclogite. *Transactions (Doklady) of the U.S.S.R. Academy of Sciences: Earth Science Sections*, 207, 121–123.

MANUSCRIPT RECEIVED JULY 30, 1999

MANUSCRIPT ACCEPTED JULY 7, 2000

PAPER HANDLED BY WILLIAM A. BASSETT